

Anomaly Detection for Belt Looseness using Motor Current Signal Imaging in Air Handling Unit

Sung Hyun Yun¹, Wonho Jung¹, Daeguen Lim¹ and Yong-Hwa Park¹

¹*Department of Mechanical Engineering, Korea Advanced Institute of Science and Technology, Daejeon, 34141, South Korea*

*tifon97@kaist.ac.kr
wonho1456@kaist.ac.kr
ldg0201@kaist.ac.kr
yhpark@kaist.ac.kr*

ABSTRACT

An air handling unit (AHU) is a critical component of heating, ventilation, and air conditioning (HVAC) systems. Slip of AHU is an intuitive key feature for monitoring a belt looseness fault of an AHU. However, fluctuating rotation speed of the motor and fan makes slip hard to monitor. Since the role of the belt is to deliver torque between the motor and fan, this leads to change of the motor current signal. This paper suggests a normal data-based anomaly detection that utilizes motor current signal imaging to identify belt looseness in AHUs. The overall process proceeds as followings: (1) converting 1-dimensional motor current signal into 2-dimensional image in the amplitude domain, (2) extracting features of normal data by applying convolutional neural networks (CNN), (3) calculating health index to detect the belt looseness fault. The technique to transform time-series current data to an image is based on its histogram. The image is obtained by the product of the histogram elements obtained from a current signal. The effect of torque load on a motor induces an amplitude modulation of the current signal. Current signal imaging based on histogram provides the fault features in a robust way. To validate the proposed method, a case study using an AHU testbed is conducted. The results demonstrate that the proposed method can detect belt looseness faults in AHU using only normal data, providing an approach for early fault detection in HVAC systems.

1. INTRODUCTION

An air handling unit (AHU) is a major subsystem of heating, ventilation, and air conditioning (HVAC) systems. Typical structure of AHU is belt-pulley system which connects driving motor and fan. However, the belt-pulley system is fragile to fatigue and wear, which leads a belt looseness fault in the system. Belt slip is induced by belt looseness. However, Yun et al. This is an open-access article distributed under the terms of the Creative Commons Attribution 3.0 United States License, which permits unrestricted use, distribution, and reproduction in any medium, provided the original author and source are credited.

since the rotation speed of motor and fan both oscillates, detection of belt looseness by slip is difficult. Therefore, other feature instead of rotation speed is required for detect the belt looseness failure. Recently, current based motor condition monitoring is studied. Belt looseness is reflected in the current signal in the shape of an oscillating load.

This paper is organized as follows: Section 2 provides a brief overview of recent deep learning application for anomaly detection and time-series signal imaging method. Section 3 presents the proposed method which consists of histogram-based signal imaging and algorithm using self-labeling technique. Section 4 describes a case study of AHU with belt looseness. Section 5 concludes the paper and extends future research.

2. A BRIEF OVERVIEW OF ANOMALY DETECTION USING SIGNAL IMAGING WITH DEEP LEARNING

2.1. Anomaly Detection with Deep Learning

The application of deep learning for anomaly detection is underway (Lei et al., 2020). Autoencoder (AE) is used to extract latent features from the input data (Ko et al., 2022, Cheng et al., 2021). AE exhibits a greater reconstruction error for anomalous data, relative to the normal data which are used during the training process. However, this assumption fails in reality since the autoencoder is capable of reconstructing both normal and abnormal data.

Generative adversarial networks (GAN) is used to solve the data imbalance problem. GAN accomplishes the task of generating similar data distributions to those of the provided training datasets, through the implementation of both generative and discriminative models (Lee et al., 2017, Ezeme et al., 2020). However, GAN-based anomaly detection model has significant limitations, including model instability and model collapse, that can be fatal to the effectiveness of the model.

Convolutional neural networks (CNN) capture spatial information, such as edges and shapes, by means of convolutional operations. CNN have demonstrated outstanding performance in the field of image recognition. Jiao et al. (2020) reviewed the usage of CNN in the area of fault diagnosis. It is known that the larger the number of layers is the better the performance is. Nevertheless, when the model becomes deeper, it may encounter the gradient vanishing problem, which can result in a decline in performance. He et al. (2016) developed ResNet to handle this problem. In the view of anomaly detection, CNN can be used for feature extractor. Jung et al. (2022) studied a simple CNN based feature extractor for anomaly detection of motor. To use CNN as a feature extractor, it is needed to make an image of time-series data.

2.2. Signal Imaging

Determining which features to utilize is a crucial decision when applying artificial intelligence techniques in fault diagnosis. Several researchers have tried to identify the most appropriate features that accurately represent the condition in fault diagnosis. Since visual information plays a critical role in human recognition, researchers have studied signal imaging as a means of representing the condition in fault diagnosis.

Time frequency representation is used as it provides time and frequency information of a given signal simultaneously. Short time Fourier transform (STFT) enables the analysis of non-stationary signals by decomposing them into their frequency content over short time intervals. It can provide information about the time varying behavior of a signal in both time and frequency domains. However, STFT has a trade-off relation between time and frequency resolution. Wavelet transform (WT) is a signal processing skill which decomposes a signal into a set of wavelets which are small waves of different frequencies and lengths. It can capture both time and frequency information at different resolution together. However, the effectiveness of WT depends on the selection of a right mother wavelet that is well-suited to the signal being analyzed.

Gu et al. (2020) used symmetric dot pattern (SDP) image for bearing fault diagnosis using vibration signal. SDP is to transform the one-dimensional signal into a pattern in the polar coordinate system. Jo et al. (2018) suggested nested scatter plot (NSP) which is a data wrangling method that uses image transformation of correlated time series data. Suh et al. (2022) used NSP image for predicting remaining useful life.

Recently, current signal imaging is used for anomaly detection of motor system. Jung et al. (2022) suggested modified recurrence plot (RP) for detecting inter-turn short circuit in the motor. RP is an image method that visualize periodic behavior of a system. RP provides visualized representation of periodic signals. When the inter-turn short circuit fault occurs, there is a distortion in the shape of the

current signal due to the change of resistance in the stator winding. RP is sensitive to these distortions in the sinusoidal waveform, allowing for the detection of minor changes in the current signal. However, since the current signal is modulated in the case of belt looseness, RP is unable to accurately represent the characteristics of this condition.

3. PROPOSED METHOD

3.1. Histogram-based Signal Imaging

Since CNN is specialized in image recognition, converting one-dimensional signal into two-dimensional image is considered. In this paper, histogram-based signal imaging is proposed.

For a measured signal \vec{x} , histogram frequency vector \vec{h} is obtained by the number of bins and the range which are hyperparameter for the histogram. The image matrix (A) is defined as follows:

$$A(i, j) = \begin{cases} h(i) \times h(j) & \text{otherwise} \\ 0 & h(i) \times h(j) \leq \epsilon \end{cases} \quad (1)$$

where $h(i)$ is the element of \vec{h} which means the number of data points in the given bin. The threshold value ϵ is selected in order to emphasize the character of the image. Figure 1 shows an example signal imaging process. Figure 1 a) is the original raw current signal \vec{x} . With predefined number of bins and range, the histogram \vec{h} is obtained and the Figure 1 b) is the plot of histogram. In Figure 1 c), the green arrows mean the x-axis of histogram which is amplitude domain. The brightness of the images represents the number of data points.

3.2. CNN for Feature Extractor and Mahalanobis Distance for Health Index

The overall anomaly detection algorithm is shown in Figure 2. In the training procedure, normal data is collected from the healthy state. Self-labeling process is a data augmentation technique to create a new label class. Since CNN is a typical example of supervised learning which requires labeled data, CNN cannot be trained by normal data only without self-labeling process. Therefore, the training dataset is composed of two class data: Normal and Self-labeled normal data. This paper uses a simple CNN architecture which consists of two convolution layers, one pooling layer, and two fully connected layers. For the first convolution layer, the kernel size is 5×5 and ReLU is used for activation function. The next convolution layer used 3×3 sized kernel and ReLU as activation function. Cross entropy loss and Adam optimizer are used for the loss function and optimizer, respectively.

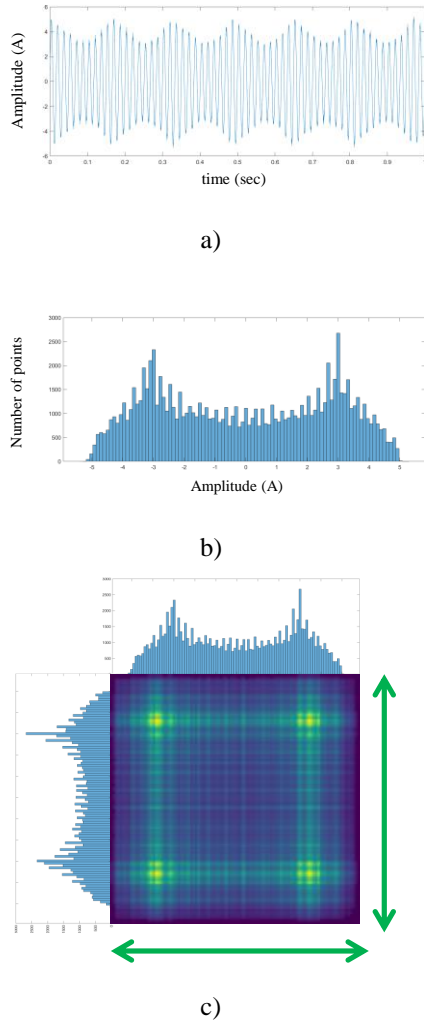


Figure 1 a) raw current signal, b) histogram of given signal, c) histogram-based image

During the training process, the training parameters are updated until the training loss converges. Once the training process is completed, the trained CNN is saved. The activation vector from the last convolutional layer of pre-trained CNN is extracted for health index.

Mahalanobis distance (MD) is a distance between a point and a distribution. Unlike Euclidean distance, MD considers the distributional information of data. MD is defined and calculated as follows:

$$MD = (x - \mu)\Sigma^{-1}(x - \mu)^T \quad (2)$$

where MD is mahalanobis distance, x is activation vector, μ and Σ is mean and covariance of saved activation map from training process. As the looseness becomes more severe, the distance tends to gradually increases from the distribution of the normal data. In this paper, health index is defined using the MD.

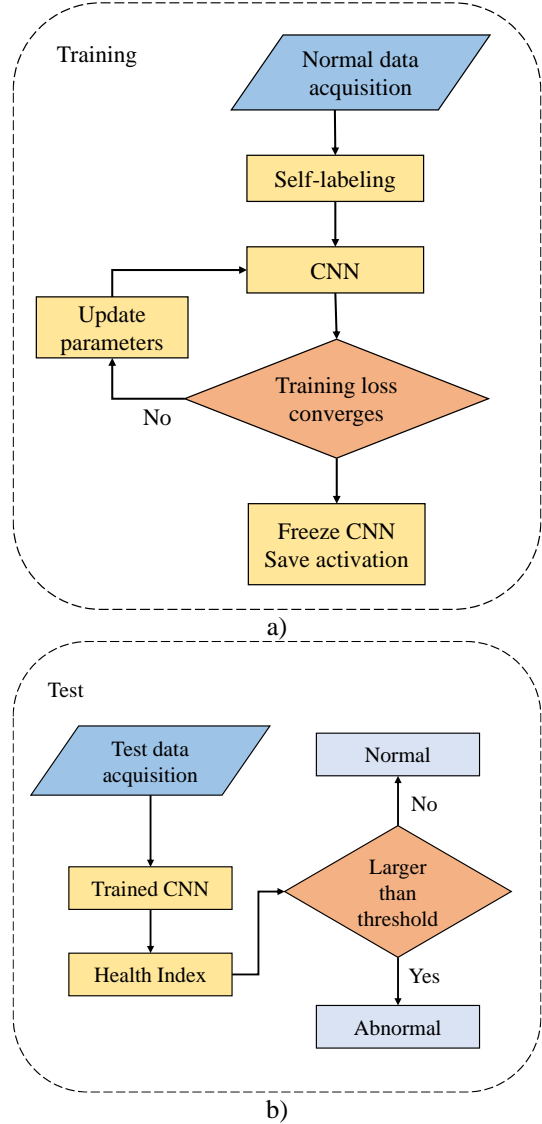


Figure 2 Framework of the proposed algorithm. a) Training process, b) Test process

4. CASE STUDY

4.1. Experimental Set up and Data Acquisition

A belt looseness simulation AHU testbed is shown in Figure 3. The testbed is composed of a commercial AHU, two encoders and three current sensors. A commercial AHU consists of several components including a motor, belt, and fan. The motor in the AHU is controlled by an inverter, which regulates its rotation speed. The motor transfers torque to the fan through a belt, which drives the rotation of the fan. The current sensors are attached to the motor. Encoder 1 is attached to get angular velocity of pulley at the motor end. Encoder 2 gets angular velocity of pulley at the fan end.

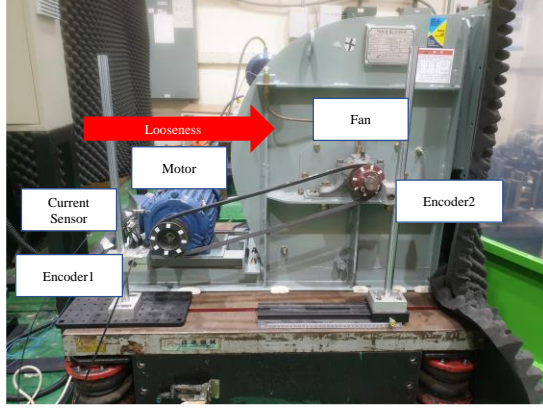


Figure 3 Testbed description

The rotation speed of the motor is 1800 RPM. The frequency of input current is 60 Hz. To simulate a belt looseness fault in an AHU testbed, the motor was moved to the right (indicated by a red arrow in Figure 3), which would cause the belt to become loose and potentially affect the performance of the fan. The default position of motor is considered as normal state, denoted as d_0 . The severity of the looseness is adjusted by changing the distance between each pulley by moving the motor to the right. Four different location, denoted as d_1 to d_4 , were examined. The examine condition is summarized in Table 1.

Table 1. Center distances and belt conditions

Center distance	Condition
d_0	Healthy belt
d_1	Weak belt looseness
d_2	Moderate belt looseness
d_3	Strong belt looseness
d_4	Critical belt looseness

To assure enough current and RPM sampling points, the sampling frequency of the current sensor and encoder is set 100kHz. Data were collected for each condition, i.e. d_0 , d_1 , d_2 , d_3 , and d_4 , for 5 minutes. To facilitate analysis, the collected data was divided into 1-second units each.

4.2. Experimental Results

The role of the belt is to transfer torque from the motor to the fan. Since the motor and fan are connected by a belt, any changes in the torque of the motor can affect the torque of the fan and vice versa. The angular velocity of fan is shown in Figure 4. As the belt looseness gets severer, the rotation speed of fan is getting lower which means that the belt cannot deliver the motor torque. To detect the belt looseness fault, slip is intuitive feature. Slip is defined and calculated by:

$$S = \left(1 - \frac{D_{fan}}{D_{motor}} \times \frac{\Omega_{fan}}{\Omega_{motor}}\right) \times 100 \quad (3)$$

where S is slip, Ω_{motor} is rotation speed of motor, Ω_{fan} is rotation speed of fan, D_{motor} is diameter of pulley at motor, and D_{fan} is diameter of pulley at fan. The diameter of each pulley is given as $D_{motor} = 6.5 \text{ cm}$ and $D_{fan} = 5.5 \text{ cm}$. The slip of each condition is shown in Figure 5. Slips of each condition overlap each other, making it challenging to distinguish between them. The images based on the proposed imaging method of each conditions are shown in Figure 6. As looseness gets worse, the edge of the image becomes thicker. Thicker edges in the image indicate weaker amplitude modulation in the current signal, which shows that load is not transferred fully due to belt looseness.

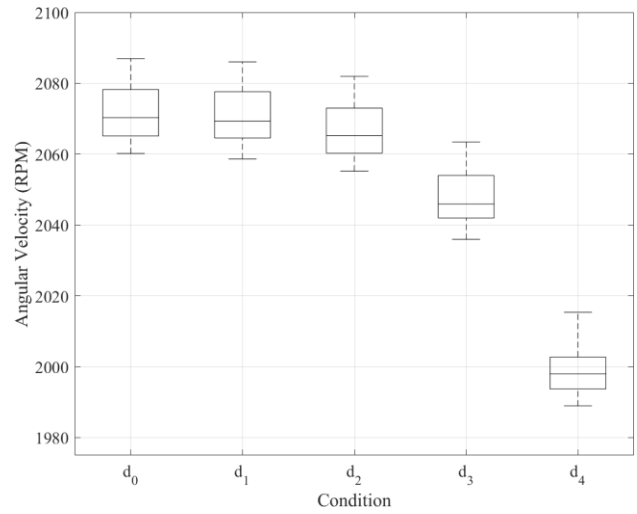


Figure 4 Angular velocity of pulley at fan end according to belt looseness condition

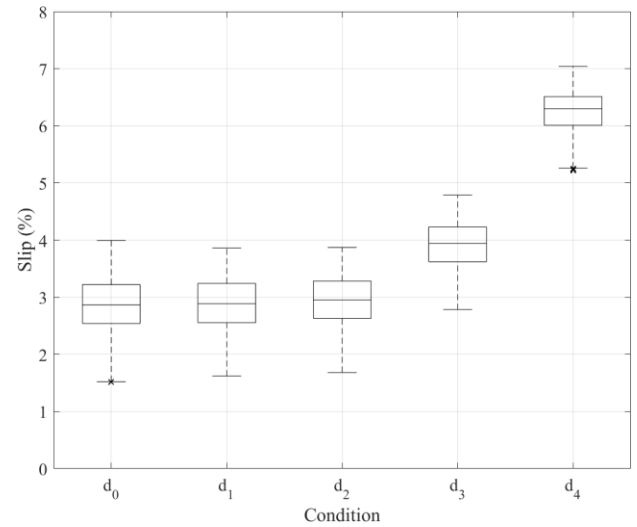


Figure 5 Slip of belt-pulley system according to belt looseness condition

To compare the performance of the proposed signal imaging method, RP image is used which is proposed by Jung et al. (2022). The RP images are shown in Figure 7. The health index of each method is shown in Figure 8. As shown in Figure 8 a), RP image cannot detect belt looseness. Low health index indicates that the RP images of each fault condition are similar to that of normal condition. However, the proposed method shows the status of belt in Figure 8 b).

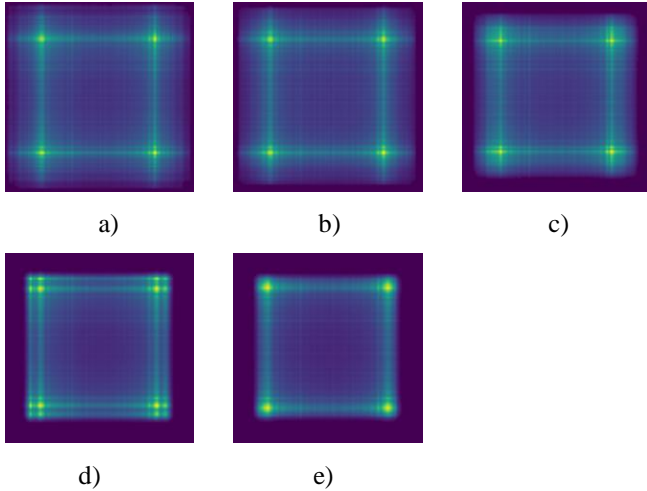


Figure 6 Proposed current signal imaging: a) healthy belt condition, b) weak belt looseness, c) moderate belt looseness, d) severe belt looseness, e) critical belt looseness

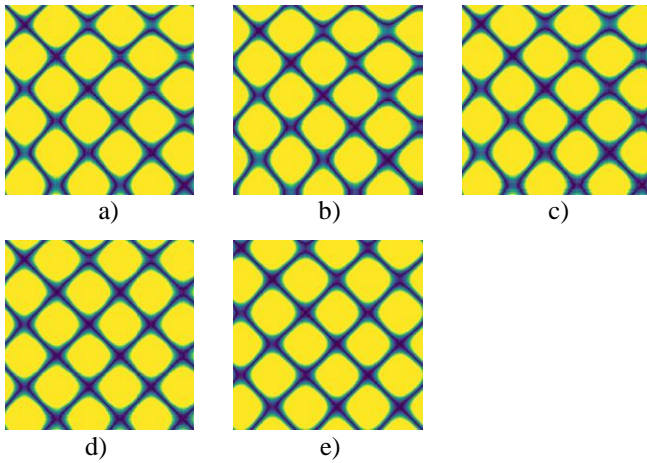


Figure 7 RP images: a) healthy belt condition, b) weak belt looseness, c) moderate belt looseness, d) severe belt looseness, e) critical belt looseness

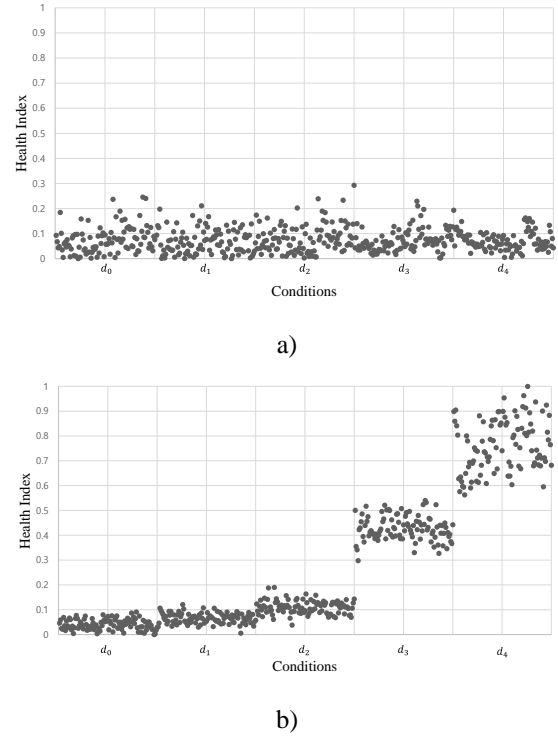


Figure 8 Health index of looseness condition: a) Recurrence plot images, b) proposed images

5. CONCLUSION

This paper presents an anomaly detection of belt looseness using current signal imaging. The proposed method is made up of three steps: (1) time-series current signal imaging based on histogram (2) extracting feature of normal state by using self-labeling and CNN (3) calculating health index using Mahalanobis distance. Current signal imaging based on histogram is applied to represent the feature of belt looseness. Self-labeling technique is also used to learn the feature of normal condition by CNN. Health index defined by MD is suggested to quantify the severity of belt looseness. The proposed method shows the possibility of detecting belt looseness with current data not pulley rotation data. Future research can extend the proposed method to detect other motors whose load is oscillating and cluster the normal distribution narrowly using contrastive loss.

REFERENCES

Lei, Y., Yang, B., Jiang, X., Jia, F., Li, N., Nandi, A. K. (2020). Applications of machine learning to machine fault diagnosis: A review and roadmap. *Mechanical Systems and Signal Processing*, vol. 138, doi:https://doi.org/10.1016/j.ymssp.2019.106587

Ko, J. U., Na, K., Oh, J., Kim, J., Youn, B. D. (2022). A new auto-encoder-based dynamic threshold to reduce false alarm rate for anomaly detection of steam turbines,

- Expert Systems With Application*, vol. 189, doi:<https://doi.org/10.1016/j.eswa.2021.116094>
- Cheng, Z., Wang, S., Zhang, P., Wang, S., Liu, X., Zhu, E. (2021). Improved autoencoder for unsupervised anomaly detection, *International Journal of Intelligent Systems*, vol.36, pp 7103-7125, doi:<https://doi.org/10.1002/int.22582>
- Lee, Y. O., Jo, J., Hwang, J. (2017). Application of Deep Neural Network and Generative Adversarial Network to Industrial Maintenance: A Case Study of Induction Motor Fault Detection. *2017 IEEE International Conference on Big Data*. December 11-14, pp 3248-3253. doi:10.1109/BigData.2017.8258307
- Ezeme, O. M., Mahmoud, O. M., Azim, A. (2020). Design and Development of AD-CGAN: Conditional Generative Adversarial Networks for Anomaly Detection. *IEEE Access*. vol. 8, pp 177667-177681, doi:10.1109/ACCESS.2020.3025530
- Jiao, J., Zhao, M., Lin, J., Liang, K. (2020). A comprehensive review on convolutional neural network in machine fault diagnosis, *Neurocomputing*, vol. 417, pp 36-63, doi:<https://doi.org/10.1016/j.neucom.2020.07.088>
- He, K., Zhang, X., Ren, S., Sun, J. (2016). Deep residual learning for image recognition. *Proceedings of the IEEE conference on computer vision and pattern recognition*. pp 770-778.
- Jung, W., Yun, S. H., Lim, Y. S., Cheong, S., Bae, J., Park, Y.H. (2022). Fault Diagnosis of Inter-turn Short Circuit in Permanent Magnet Synchronous Motors with Current Signal Imaging and Semi-Supervised Learning. *IECON 2022-48th Annual Conference of the IEEE Industrial Electronics Society*. October 17-20, doi:10.1109/IECON49645.2022.9968718
- Gu, Y., Zeng, L., Qiu, G. (2020). Bearing fault diagnosis with varying conditions using angular domain resampling technology, SDP and DCNN. *Measurement*. vol. 156, pp 107616. doi:<https://doi.org/10.1016/j.measurement.2020.107616>
- Jo, J., Lee, Y. O., Hwang, J. (2018). Multi-Layer Nested Scatter Plot a Data Wrangling Method for Correlated Multi-Channel Time Series Signals. *2018 First International Conference on Artificial Intelligence for Industries (AI4I)*. pp 106-107.
- Suh, S., Lukowicz, P., Lee, Y. O. (2022). Generalized multiscale feature extraction for remaining useful life prediction of bearings with generative adversarial networks. *Knowledge-Based Systems*. vol. 237, pp 107866, doi:<https://doi.org/10.1016/j.knosys.2021.107866>
- Sung Hyun Yun** received the B.S. degree in mechanical engineering from Hanyang University, Seoul, South Korea, in 2022. He is currently pursuing the M.S. degree in mechanical engineering from Korea Advanced Institute of Science and Technology, Daejeon, South Korea. His current research interests include deep learning-based prognostics and health management for machinery and structures.
- Wonho Jung** received the B.S. degree in electronic engineering from Gachon University, Seongnam, South Korea, in 2020. He works as a researcher in Korea Advanced Institute of Science and Technology, Daejeon, South Korea. His current research topics include deep learning-based prognostics and health management for machinery and structures.
- Daeguen Lim** received the B.S. and M.S. degree in mechanical engineering from Pusan National University, Busan, South Korea, in 2012 and 2014, respectively. He worked as a researcher at MIDASIT in Seongnam, South Korea from 2014 to 2016. From 2016 to 2021, he worked as a senior researcher at LG Electronics in Changwon, South Korea and Hyundai Heavy Industry in Ulsan, South Korea. He is currently pursuing the Ph.D. degree in mechanical engineering from Korea Advanced Institute of Science and Technology, Daejeon, South Korea. His current research topics include reduced-order modeling for constructing high-fidelity digital twins of machinery and structures.
- Yong-Hwa Park** received the B.S., M.S. and Ph.D. degrees in mechanical engineering from the Korea Advanced Institute of Science and Technology, Daejeon, South Korea, in 1999. From 2000 to 2003, he was a postdoctoral research associate with aerospace engineering department of University of Colorado, Boulder, supervised by Prof. K. C. Park. From 2012 to 2016, he was a research master with the Samsung Advanced Institute of Technology (SAIT), Samsung Electronics, Suwon, South Korea. Since 2016, he has been an Associate Professor with the Korea Advanced Institute of Science and Technology. His research interests, in 1999. From 2000 to 2003, he was a postdoctoral research associate with aerospace engineering department of University of Colorado, Boulder, supervised by Prof. K. C. Park. From 2012 to 2016, he was a research master with the Samsung Advanced Institute of Technology (SAIT), Samsung Electronics, Suwon, South Korea. Since 2016, he has been an Associate Professor with the Korea Advanced Institute of Science and Technology. His research interests include vibration modeling/analysis, acoustic event detection, biometric recognition by human body vibration, and 3D shape/motion measurement.